

Constraining the orbital orientation of η Carinae from H Paschen lines

D. Falceta-Gonçalves^{1*} and Z. Abraham²

¹*Núcleo de Astrofísica Teórica, Universidade Cruzeiro do Sul, Rua Galvão Bueno 868, 01506-000, São Paulo, Brazil*

²*Instituto de Astronomia, Geofísica e Ciências Atmosféricas, Universidade de São Paulo - Rua do Matão 1226, 05508-090, São Paulo, Brazil*

ABSTRACT

During the past decade several observational and theoretical works provided evidences of the binary nature of η Carinae. Nevertheless, there is still no direct determination of the orbital parameters, and the different current models give contradictory results. The orbit is, in general, assumed to coincide with the Homunculus equator although the observations are not conclusive. Among all systems, η Carinae has the advantage that it is possible to observe both the direct emission of line transitions in the central source and its reflection by the Homunculus, which are dependent on the orbital inclination. In this work, we studied the orbital phase dependent hydrogen Paschen spectra reflected by the SE lobe of the Homunculus to constrain the orbital parameters of η Car and determine its inclination with respect to the Homunculus axis. Assuming that the emission excess is originated in the wind-wind shock region we were able to model the latitude dependence of the spectral line profiles. For the first time, we were able to estimate the orbital inclination of η Car with respect to the observer and to the Homunculus axis. The best fit occurs for an orbital inclination to the line of sight of $i \sim 60^\circ \pm 10^\circ$, and $i^* \sim 35^\circ \pm 10^\circ$ with respect to the Homunculus axis, indicating that the angular momenta of the central object and the orbit are not aligned. We were also able to fix the phase angle of conjunction as $\sim -40^\circ$, showing that the periastron passage occurs shortly after conjunction.

Key words: stars: individual: η Carinae – stars: binaries: general – stars: winds

1 INTRODUCTION

Among the most massive and luminous stars in the Galaxy η Carinae is possibly the most enigmatic and intriguing object. Unique features, e.g. variable emissions and the outbursts that occurred during the 1800's, which generated the Homunculus - the giant bipolar gas structure surrounding the star -, made difficult the understanding of the real nature of this object. Its periodicity in the observed light curves and spectral lines at all wavelengths indicated its binary nature with $P = 5.52$ years (Damineli 1996, Corcoran et al. 2001, Stahl et al. 2005).

From the X-ray light curve and spectra it is possible to infer the existence of a strong wind-wind shock, expected for an O-type or Wolf-Rayet (WR) companion star (Pittard & Corcoran 2002). However, since there is no direct observation of the individual stars of the system it is difficult to precisely derive its orbital parameters, e.g. the eccentricity, inclination and periastron position, and indirect methods have to be used. The periodic variations in the X-ray light curve, which is originated by the wind-wind shocked

gas during periastron passage, has already provided some clues on this issue (Corcoran 2005). Similarly, the sharp drop in flux has also been observed at optical (Fernández-Lajús et al. 2008), infrared (Whitelock et al. 2004) and radio wavelengths (Duncan & White 2003, Abraham et al. 2005a), but with different duration. Corcoran et al. (2001) assumed that the "eclipse-like" dips are produced by increased absorption in the stellar envelope. In this scenario, the orbital plane should closely intercept the line of sight and the periastron should be located in opposition regarding the observer. Falceta-Gonçalves, Jatenco-Pereira & Abraham (2005) proposed a different scenario, in which the remnant post-shocked gas could increase the optical depth and explain the observed X-ray light curve if the periastron passage is close to conjunction. In a further work, it was also possible to reproduce the radio light curves under this assumption (Abraham et al. 2005b). The same process could be invoked to explain the decrease in optical and infrared fluxes.

Although X-rays, optical, infrared, and radio light curves may provide clues on the orbit of the system, and even be used on the accurate estimation of the stellar wind properties, it is well known that modelling spectral line pro-

* e-mail:diego.goncalves@cruzeirosul.edu.br

files is the best method to determine orbital parameters of binary systems, in general, with good precision.

Damineli (1996), studying the HeI λ 10830, reported a periodicity of 5.5yrs in the spectroscopic events, the epochs in which the line disappear. Steiner & Damineli (2004) studying the higher excitation energy lines of He II, on the other hand, reported a peak in intensity right before periastron passage. Compared to the X-ray light curve, the similarity reveals that they may have the same origin. Further studies, with higher resolution spectra (Martin et al. 2006), have shown that, not only the line intensities vary within the 5.5yrs period, but also their profiles. They concluded that the line source might be more complex than simply atmospheric emission, and the decline in flux cannot be explained only by eclipsing models. Nielsen et al. (2007) attempted to explain the line-profiles assuming that the emission is the combination of a major component originated in the stellar wind, and other minor contributions at different velocities, which origin is not clear. From the line velocity curve, they inferred an eccentricity $e \sim 0.9$, and that periastron should be placed near opposition.

Falceta-Gonçalves, Jatenco-Pereira & Abraham (2007) showed that line profile variability is expected from emission originated in the wind-wind interaction zone. Its study showed to be a powerful tool in determining the orbital parameters of WR30a (Falceta-Gonçalves, Abraham & Jatenco-Pereira 2008), where by fitting synthetic profiles to the observational data, it was possible to determine the inclination and eccentricity of the orbit. Also, using the line velocities obtained directly from the primary O-star, it was possible to constrain the stellar masses.

In the η Carinae binary system, observations of direct and Homunculus reflected emission show multi-peaked spectral lines, with profiles and intensities that vary with orbital phase. Stahl et al. (2005) showed that the HeII λ 4686Å emission lines measured towards the central object and the SE lobe of the Homunculus presented different profiles, in contradiction to what would be expected assuming spherical symmetry. Abraham & Falceta-Gonçalves (2007) showed that the conical wind-wind shock region could be the main source of the observed excess in the HeII λ 4686Å line profiles. To reproduce both the direct and Homunculus reflected line profiles it was necessary to assume that the Homunculus axis does not coincide with the axis of the orbital plane. However, due to the limited amount of data, which were restricted to orbital phases very close to periastron passage, it was not possible to lift the degeneracy regarding the inclination of the orbital and Homunculus axis. In all cases, the observed velocity curve, as well as the line profiles, are well reproduced only if periastron occurs near conjunction.

In the present work we extended the analysis of Abraham & Falceta-Gonçalves (2007), applying this model to the H Paschen 8 line reflected by the Homunculus SE lobe observed by Stahl et al. (2005) and derive, for the first time, the orbital and Homunculus axis inclination. In Section 2 we describe the model and the adopted geometry for the system; in Section 3 we show the results, followed by the conclusions in Section 4.

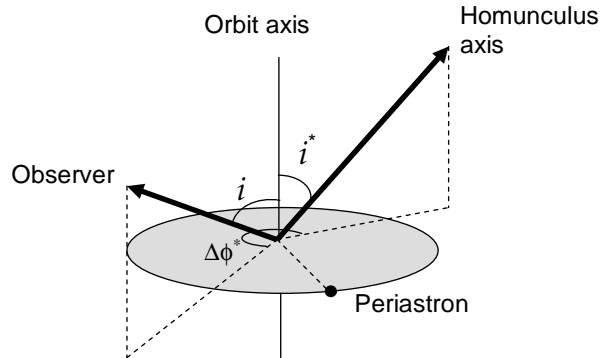


Figure 1. Scheme of the system geometry. The orbital axis has an inclination i regarding the line of sight and i^* regarding the Homunculus axis. It is assumed that the angle between the line of sight and Homunculus axis is of 45° (Davidson et al. 2001, Smith et al. 2004).

2 MODEL

As the massive and supersonic winds of the two stars collide, they create a wind-wind interaction region, structured as two shocks at both sides of the contact discontinuity where the wind momenta are equal. As described in Luo, McCray & Mac-Low (1990), the geometry of the contact discontinuity is asymptotically conical, with an opening angle β given by:

$$\beta \simeq 120^\circ \left(1 - \frac{\eta^{2/5}}{4} \right) \eta^{1/3}, \quad (1)$$

where $\eta = \dot{M}_s v_s / \dot{M}_p v_p$, \dot{M}_p and \dot{M}_s are the mass loss rates and v_p and v_s the wind velocities of the primary and secondary stars, respectively.

At the shock surfaces the compressed gas reaches temperatures of $\sim 10^6 - 10^8$ K and emits free-free radiation, mostly at X-ray wavelengths. As this gas flows along the shock structure, it cools down to recombination temperatures and becomes denser (Abraham et al. 2005a,b; Falceta-Gonçalves, Jatenco-Pereira & Abraham 2005). At this stage, it could possibly be the source of He and H lines, explaining some of the features observed in the spectra of massive binary systems (Falceta-Gonçalves, Abraham & Jatenco-Pereira 2006, 2007).

The model, proposed in Falceta-Gonçalves et al. (2006), considers the emission from each subvolume of the conic shaped shock structure between the stars. The line intensity is obtained by the integration of each fluid element emission along the line of sight:

$$I(v) = \mathcal{C}(\varphi) \int_0^\pi \exp \left[-\frac{(v - v_{\text{obs}})^2}{2\sigma^2} \right] e^{-\tau(\alpha)} d\alpha, \quad (2)$$

where $v_{\text{obs}} = v_{\text{flow}} (-\cos \beta \cos \varphi \sin i + \sin \beta \cos \alpha \sin \varphi \sin i - \sin \beta \sin \alpha \cos i)$, is the observed stream velocity component projected into the line of sight, α the azimuthal angle of the shock cone, i the orbital inclination, φ the orbital phase angle, σ the turbulent velocity amplitude, τ the optical depth along the line of sight and $\mathcal{C}(\varphi)$ a normalization constant.

From Eq. 2, it is possible to obtain synthetic line profiles and compare them to the observations, as it was done with the HeII λ 4686Å emission line (Abraham & Falceta-

Table 1. Parameters and input values

parameter	input value	reference
e	0.95	Abraham et al. (2005b)
ϕ_0	-40°	Abraham & Falceta-Gonçalves (2007)
P	2024 days	Corcoran (2005)
a	15A.U.	Falceta-Gonçalves et al. (2005)
t_0	2,450,795 JD	Abraham et al. (2005b)
β	45°	Abraham & Falceta-Gonçalves (2007)
$v_{\text{flow}} \sin \beta$	450 km s^{-1}	Abraham & Falceta-Gonçalves (2007)
σ	$0.33v_{\text{flow}}$	Abraham & Falceta-Gonçalves (2007)

Gonçalves 2007). To fit the lines reflected by the Homunculus, it is also necessary to take into account the angle between the Homunculus axis and the line of sight Ψ , and the inclination of the Homunculus axis with respect to the orbital plane.

In Fig. 1 we describe the geometry of the system as we assumed in the model. Here, i and i^* represent the inclination of the LOS and of the Homunculus axis with respect to the orbital axis, respectively. In this case, we may write the relationship between these angles as:

$$\cos \Psi = \sin i \sin i^* \cos \Delta\phi^* + \cos i \cos i^*, \quad (3)$$

where $\Delta\phi^*$ represents the angle between the projection of the Homunculus axis into the orbital plane and the line of sight. Following Davidson et al.(2001) and Smith et al. (2004), we will consider the angle between the Homunculus axis and the LOS close to $\Psi \sim 45^\circ$.

3 OBSERVATIONAL DATA

Stahl et al. (2005) presented VLT/UVES observations of the line emission reflected by the SE lobe of the Homunculus, carried out from December 2002 to March 2004, or phase interval between 0.9 and 1.127, including the minimum event of 2003.5. The Paschen P8 line profile presented strong variability, with clear P Cygni absorption, probably related to the stellar wind. Also, in all observations, two prominent excess emission bumps are visible, which we interpreted as extra emission from the shock region. The digitalized excess emission velocity profiles are shown in Figure 2 as filled circles, corrected by the expansion velocity of the Homunculus $V = 100 \text{ km s}^{-1}$. The numbers at each spectrum represent the date of the observation (JD - 2.400.000).

The observed peaks reflected by the Homunculus pole occurred at $v \sim 0 \text{ km s}^{-1}$ and $v \sim +220 \text{ km s}^{-1}$, while direct observations towards the central star revealed $v \sim 0$ and $v < 150 \text{ km s}^{-1}$ (Weis et al. 2005). This difference shows that, at least part of the observed emission has an anisotropic origin. We assumed that this latitude dependence is connected to the emission from the conic shock region.

4 RESULTS

We applied the model described in the Section 2 to the observational data. For the wind parameters we used $\dot{M}_p =$

$2.5 \times 10^{-3} M_\odot \text{ yr}^{-1}$, $v_p = 700 \text{ km s}^{-1}$, $\dot{M}_s = 5 \times 10^{-5} M_\odot \text{ yr}^{-1}$, $v_s = 3000 \text{ km s}^{-1}$, which results in $\eta = 0.1$ and, from Eq. 1, we obtain $\beta = 45^\circ$. For the flow along the conic surface we assumed $v_{\text{flow}} \sin \beta = 450 \text{ km s}^{-1}$ and $\sigma = 0.33v_{\text{flow}}$ (Abraham & Falceta-Gonçalves 2007). Because of the size of the Homunculus, we must also take into account the delay in the light travel from the wind-wind interaction zone to the reflection nebula. The data obtained from the reflection of the expanding nebula corresponds to an emission that occurred in a phase previous than that observed directly towards the central star. This delay is particularly important for this model because a difference in the phase of the emission corresponds in a difference in the orientation of the shock cone regarding the Homunculus and, therefore, a difference shift velocity. The time delay may be calculated as:

$$\frac{t_{\text{delay}}}{c} \sim \frac{t_{\text{expansion}}}{v_{\text{expansion}}}, \quad (4)$$

considering an expansion of 100 km s^{-1} since the outburst about 160 years ago, we get $t_{\text{delay}} \sim 20$ days. Therefore, in order to precisely fit the model, we must subtract 20 days in the orbital phase and determine the actual orientation of the shock cone for the given phase angle. For the determination of the orbital phases we used the epoch of conjunction as June 29, 2003 (Abraham et al. 2005b), $e = 0.95$ and an angle between periastron and conjunction $\phi_0 = 40^\circ$ (Abraham & Falceta-Gonçalves 2007)

In Table 1 we show the input parameters of the model and their corresponding values. In the present work the input parameters, shown in Table 1, are fixed. We will briefly discuss the role of each of them on the obtained results later in the paper. Finally, we fitted the observational data using Eq. 2, together with Eq. 3, for an optically thin gas ($\tau \sim 0$). In Falceta-Gonçalves et al. (2007) it has been shown that optically thick wind-wind shocks result in single peaked profiles, while the data of Paschen lines of η Car presented double-peaked profiles at all phases. In order to obtain the best fitting set of values of i and i^* , we calculate the synthetic line profiles for the observed epochs for the range -180° to 180° , independently for i and i^* , in steps of $\Delta i = 10^\circ$. The observed data and three of the best models we fitted are shown in Fig. 2. The lines represent the models for different values of i and i^* . It is noticeable from the modeled spectra that the line profiles are very sensitive to changes in the orbital inclination regarding both the observer and the Homunculus. The best fit, i.e. the minimum cumulative error for all orbital phases, is obtained for $i^* \sim 35^\circ \pm 10^\circ$ and $i \sim 60^\circ \pm 10^\circ$, i.e. an angle between the orbital plane and the line of sight of $\sim 30^\circ$, in agreement with the radio detection of the almost edge-on gas disk formed around the system. Note that the error of $\Delta i = 10^\circ$ represents the ‘‘resolution’’ of the sets of i and i^* that we have calculated. Due to a small degeneracy between i and i^* for small values of Δi , it is not possible to reduce the imprecision in the determination of these parameters.

The most important issue regarding these results is that the Homunculus and the orbital plane axis are not aligned, as usually assumed (see Steiner & Damineli 2004, Martin et al. 2006, Okazaki et al 2008). Since the Homunculus is assumed to be coincident with the stellar rotation axis at the epoch when the outburst event occurred, we may con-

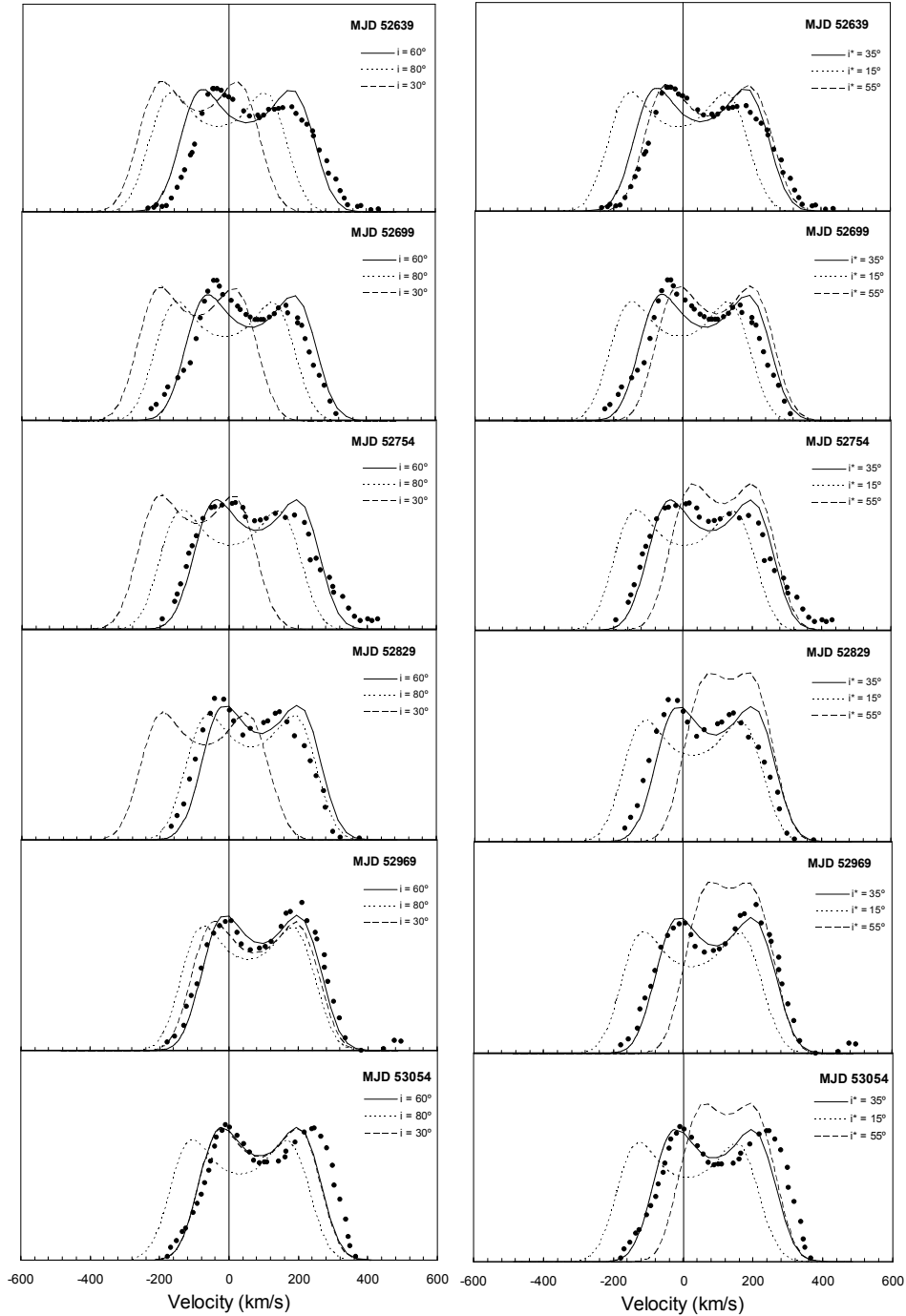


Figure 2. Time series of the Paschen 8 line profiles, after continuum subtraction, measured for the Homunculus SE lobe. *Left:* the lines show the modeled line profiles for $i^* = 35^\circ$ and orbital inclinations regarding the line of sight $i = 30^\circ$ (dashed), 60° (solid) and 80° (dotted). *Right:* the lines show the modeled line profiles for $i = 60^\circ$ and orbital inclinations regarding the Homunculus axis $i^* = 55^\circ$ (dashed), 35° (solid) and 15° (dotted).

clude that the stellar and orbital momenta were not parallel (or even close to that). Considering other massive binary systems, it is well known that the relaxation timescales for close binary systems are short, of order of hundred to a few thousands of years (e.g. Tassoul 1990). *Should we expect the orbital and stellar angular momenta to coincide after the stellar evolution ($\sim 10^6$ yr) due to tidal relaxation?*

4.1 Relaxation timescales

Close massive binary systems are known to present strong tidal torques (Lecar, Wheeler & McKee 1976), which result in i-) orbital circularization, ii-) stellar rotation synchronization with the orbital period and iii-) alignment of stellar and orbital angular momenta. The last is particularly important considering the results obtained in this work.

To verify the plausibility of a non-aligned orbital and

stellar momenta scenario, we may estimate the relaxing timescale of the η Carinae system. Several authors have addressed the problem in the past (e.g. Zahn 1977, Hut 1982, Eggleton, Kiseleva & Hut 1998). The gravitational pull force acting on each star results in the non-spherical distribution of the stellar mass. However, since the stars are moving fast in close binaries, the orientation of the tides are not coincident with the direction of the centers of mass. The extra force component is responsible for the net torque that changes the energy and angular momentum of the orbital motion and stellar rotation.

In particular, Hut (1982) studied the dynamical evolution of close binary systems with high eccentricity due to tidal friction between the two stars - a scenario we believe is correct for η Carinae. In the case of high eccentricity, and a ratio of rotation to orbital angular momenta $\kappa \ll 1$, the orbital and stellar angular momenta tend to become parallel for timescales of order:

$$\tau_{\text{align}} \sim 0.02T \left(\frac{D}{R_p}\right)^6 \left(\frac{r_g}{q}\right)^2 \frac{\Omega_p}{k\omega_p} \epsilon^{-3/2} (2-\epsilon)^{13/2}, \quad (5)$$

where k is the apsidal motion constant, D is the distance between the stars at periastron passage, $q = M_s/M_p$ is the ratio between the stellar masses, $\epsilon = (1-e)$, $r_g = [I_p/(M_p R_p^2)]^{1/2}$, I_p is the moment of inertia, Ω_p the angular velocity and R_p the radius of the primary star,

$$\omega_p = [G(M_p + M_s)(1+e)]^{1/2} D^{-3/2}, \quad (6)$$

is the orbital angular velocity at periastron, and:

$$T = \frac{R_p^3}{GM_p \tau}, \quad (7)$$

where τ is the constant time lag of the tidal axis with respect to a coordinate system corotating with the primary star. The apsidal motion constant k depends on the internal structure of the star, and is typically of the order of $10^{-3} - 10^{-1}$.

From Eqs. 5-7 it is clear that the relaxing timescale of the system depends on several poorly known parameters, though an estimation is still possible. For $D \sim 10R_p$, $r_g/q \sim 1$, $M_s/M_p \sim 0.4$, $\Omega_p \sim \omega_p$ and $T \sim 10^8$ s we have $\tau_{\text{align}} \sim 10^{16} - 10^{18}$ s, or $\sim 10^8 - 10^{10}$ yr, for $k = 10^{-3} - 10^{-1}$. From the parameters used in this estimation, the ratio Ω_p/ω_p is the main unknown. Typically, we would expect a ratio ~ 1 for a relaxed system, but a ratio > 1 for a young wide binary system. In this case, the relaxation timescale would be even larger and our conclusions unchanged.

Typically, the lifetime of stars with $M > 60M_\odot$ is 1 – 5 Myr (Schaller et al. 1992). Therefore, we may conclude that η Carinae system, during its evolution up to the outburst in the 19th century, had not enough time to relax, and we should not expect the orbital and rotation angular momenta to be aligned. Interestingly, this also reveals that the orbital high eccentricity ($e > 0.9$) may be primordial, even though it could also be a result of the massive mass ejection events.

5 CONCLUSIONS

Although many authors agree about the binary nature of η Carinae, its orbital parameters and orientation are still poorly known. From the X-ray and radio light curves, as well as the spectral line velocity curves, it is possible to derive

high eccentricity ($e > 0.9$) (Ishibashi et al. 1999, Abraham et al. 2005b, Falceta-Gonçalves, Jatenco-Pereira & Abraham 2005). Also, from the spectral line profiles it was believed that the periastron should happen in opposition to the observer, with $\phi_0 = 270^\circ$, if one assumes that the emission comes exclusively from the stellar winds (Davidson 1997, Nielsen et al. 2007). Abraham & Falceta-Gonçalves (2007) showed that the wind-wind shock region can be responsible for the HeII4686 emission excess, and consistently fit the observed spectra. However, in this case the periastron should occur near conjunction instead ($\phi_0 = 40^\circ$).

Regarding the orbital inclination, it is commonly assumed that the orbital plane should be nearly aligned with the Homunculus equator (Davidson 1997, Smith et al. 2004), which is inclined $\sim 45^\circ$ with respect to the observer. In contradiction to that, high resolution radio observations show the presence of a gas torus surrounding the system, which seems to be seen edge-on (Duncan & White 2003), indicating that the orbit may not be aligned with the Homunculus. In this scenario, the torus would also be responsible for the shell-like effect seen in the X-ray light curve (Falceta-Gonçalves, Jatenco-Pereira & Abraham 2005).

In this work we studied the possibility of the orbital plane and the Homunculus not being aligned. For that, we used the hydrogen Paschen 8 line spectral profiles obtained from the SE lobe of the Homunculus. This line is supposed to originate in the central system and reflected by the expanding gas. The observed excess flux presented two peaked line profiles, which velocities change with the orbital phases. This behaviour is common in massive binary systems where the line emission originates in the wind-wind interaction zone. The conical shock surface would be responsible for an anomalous two peaked profile with velocities changing during the orbital period as the line of sight is intercepted by different vector projections of the flowing gas, as detailed in Falceta-Gonçalves, Abraham & Jatenco-Pereira (2006).

We applied the synthetic line profile model, considering the emission from the central system, and derived the reflected fluxes at the SE lobe of the Homunculus. We fixed the stellar and orbital parameters $\beta = 45^\circ$, $e = 0.95$, $v_{\text{flow}} \sin \beta = 450 \text{ km s}^{-1}$, $\phi_0 = -40^\circ$ and $\sigma = 0.33v_{\text{flow}}$ (Abraham & Falceta-Gonçalves 2007), and left the orbital inclination regarding the line of sight (i) and regarding the Homunculus axis (i^*) as fit parameters. We showed that the line profiles are very sensitive to changes in the orbital inclination regarding both the observer and the Homunculus axis. Therefore, this method has revealed helpful in constraining the orbital orientation of the system. The best fit was obtained for $i \sim 60^\circ \pm 10^\circ$ and $i^* \sim 35^\circ \pm 10^\circ$. This result shows that the line of sight must lie close to the orbital plane ($i \sim 30^\circ$), as indicated by radio observations and theoretical models regarding the X-ray light curve.

In the presented calculations, most of the orbital and stellar parameters were fixed, based on previous references (Table 1). It is important though to understand if changes in any of these would reflect in major changes on our results and conclusions. The eccentricity of the orbit is a well-known parameter as it is constrained by the velocity curves of several spectral lines - we should expect its value to vary within the range $e = 0.9 - 0.95$. A different eccentricity would simply change the orbital phase, in which a given synthetic line would fit the data, therefore being irrelevant

for the synthetic profiles. The same occurs for ϕ_0 , P , a and t_0 . Actually, ϕ_0 is also related to the curvature of the shock cone. The turbulence amplitude σ , on the other hand, is responsible for the broadness of the synthetic line profiles. Since the observed broadness for each peak is unchanged at different orbital phases, its value is also irrelevant on the determination of i and i^* . It is important though to remember that σ presents a degeneracy with v_{flow} , i.e. if the system has a smaller value of v_{flow} , we would need a larger value of σ to account for the same line broadness being v_{flow} directly obtained from the observed line velocities, but it has no influence on the determination of the inclination of the orbital plane. Among the fixed parameters, β is the only strongly correlated with i and i^* . As fully discussed in Falceta-Gonçalves et al. (2006), a sequence of synthetic profiles may be well reproduced if an increased value of β is balanced by a decrease of i , regarding the line of sight. However, considering the observed profiles, this degeneracy is limited to the range in which $i < \beta$ because, otherwise, models with $i > \beta$ result in single peaked profiles in certain orbital phases. Since the observational data presents two-peaked profiles in all phases we may constrain $i < \beta$. Fortunately, β depends on the stellar winds of the two stars, which are approximately well constrained to provide $\beta \sim 40^\circ - 50^\circ$. This range of possible β values is coherent with the obtained range of $i \sim 30^\circ \pm 10^\circ$, regarding the line of sight.

Also, the results show that the Homunculus axis is not perpendicular to the orbital plane. This suggests that the stellar angular momentum, probably coincident with the Homunculus axis, is not aligned with the orbital motion. We explained this fact showing that the relaxing timescale for momenta alignment and orbital circularization of η Carinae is longer than the stellar lifetime. This fact also explains the high eccentricity of the system ($e \sim 0.95$), since tidal interactions did not have enough time to circularize the orbit. It is true though that the outburst occurred in the 19th century could have been responsible for large changes in the orbital parameters as well.

Finally, direct observations toward the central star revealed an increase in P Cygni absorption during the minimum (Davidson et al. 2005), as opposed to the polar data, which shows almost constant absorption. This fact tells us that the main responsible for this absorption is not the primary star wind but, if the orbital plane is close to the LOS, the secondary star wind or the remaining post-shocked gas within the star and the observer.

ACKNOWLEDGMENTS

D.F.G thanks FAPESP (No. 06/57824-1) and CNPq for financial support. Z.A. thanks FAPESP, CNPq and FINEP for support.

REFERENCES

Abraham, Z., Falceta-Gonçalves, D., Dominici, T. P., Nyman, L.-A., Durouchoux, P., McAuliffe, F., Caproni, A. & Jatenco-Pereira, V. 2005, *A&A*, 437, 997
 Abraham, Z., Falceta-Gonçalves, D., Dominici, T.,

Caproni, A. & Jatenco-Pereira, V. 2005, *MNRAS*, 364, 922
 Abraham, Z. & Falceta-Gonçalves, D. 2007, *MNRAS*, 378, 309
 Corcoran, M. F., Ishibashi, K., Swank, J. H. & Petre, R. 2001, *ApJ*, 547, 1034
 Corcoran, M. F. 2005, *AJ*, 129, 2018
 Damineli, A. 1996, *ApJ*, 460, 49
 Davidson K. 1997, *New Astr.*, 2, 387
 Davidson K., Smith N., Gull T. R., Ishibashi K. & Hillier D. J. 2001, *AJ*, 121, 1569
 Davidson, K., Martin, J., Humphreys, R. M., Ishibashi, K., et al. 2005, *AJ*, 129, 900
 Duncan, R. A. & White, S. M. 2003, *MNRAS*, 338, 425
 Eggleton, P. P., Kiseleva, L. & Hut, P. 1998, *ApJ*, 499, 853
 Falceta-Gonçalves, D., Jatenco-Pereira, V. & Abraham, Z. 2005, *MNRAS*, 357, 895
 Falceta-Gonçalves, D., Abraham, Z. & Jatenco-Pereira, V. 2006, *MNRAS*, 371, 1295
 Falceta-Gonçalves, D., Abraham, Z. & Jatenco-Pereira, V. 2007, *IAUS*, 240, 198
 Falceta-Gonçalves, D., Abraham, Z. & Jatenco-Pereira, V. 2008, *MNRAS*, 383, 258
 Fernández-Lajús, E., Fariña, C., Torres, A. F., Schwartz, M. A. et al. 2008, *A&A*, accepted
 Hut, P. 1982, *A&A*, 110, 37
 Ishibashi K. Corcoran M., Davidson K., Swank J., Petre R., Drake S., Damineli A. & White S. 1999, *ApJ*, 524, 983
 Lecar, M., Wheeler, J. C. & McKee, C. F. 1976, *ApJ*, 106, 221
 Luo, D., McCray, R. & Mac-Low, M. 1990, *A&A*, 383, 636
 Martin, J. C., Davidson, K., Humphreys, R., Hillier, D. J. & Ishibashi, K. 2006, *ApJ*, 640, 474
 Nielsen, K. E., Corcoran, M. F., Gull, T. R., Hillier, D. J., Hamaguchi, K., Ivarsson, S. & Lindler, D. J. 2007, *ApJ*, 660, 669
 Pittard, J. M. & Corcoran, M. F. 2002, *ApJ*, 362, 267
 Okazaki, A. T., Owocki, S. P., Russell, C. M. P. & Corcoran, M. F. 2008, *MNRAS*, 388, 39
 Schaller, G., Schaerer, D., Meynet, G. & Maeder, A. 2004, *A&A*, 96, 269
 Smith N., Morse J. A., Collins N. R. & Gull T. R. 2004, *ApJ*, 610, 105
 Stahl, V., Weis, K., Bomans, D. J., Davidson, K., Gull, T. R. & Humphreys, R. M. 2005, *A&A*, 435, 303
 Steiner, J. E. & Damineli, A. 2004, *ApJ*, 612, 133
 Tassoul, J.-L. 1990, *ApJ*, 358, 196
 Weis, K., Stahl, O., Bomans, D. J., Davidson, K., Gull, T. R., Humphreys, R. M. 2005, *AJ*, 129, 1694
 Whitelock, P. A., Feast, M.W., Marang, F., & Breedt, E. 2004, *MNRAS*, 352, 447
 Zahn, J.-P. 1977, *A&A*, 57, 383